PNAS RESEARCH ARTICLE | NEUROSCIENCE OPEN ACCESS

Semaphorin 1a-mediated dendritic wiring of the *Drosophila* mushroom body extrinsic neurons

Chen-Han Lin[a,b], Bhagyashree Senapati[b,1], Wen-Jie Chen[b,c], Sonia Bansal[b,d], and Suewei Lin[a,b,2]

Edited by Claude Desplan, New York University, New York, NY; received June 25, 2021; accepted February 3, 2022

The *Drosophila* mushroom body (MB) is composed of parallel axonal fibers from intrinsic Kenyon cells (KCs). The parallel fibers are bundled into five MB lobes innervated by extrinsic neurons, including dopaminergic neurons (DANs) and MB output neurons (MBONs) that project axons or dendrites to the MB lobes, respectively. Each DAN and MBON innervates specific regions in the lobes and collectively subdivides them into 15 zones. How such modular circuit architecture is established remains unknown. Here, we followed the development of the DANs and MBONs targeting the vertical lobes of the adult MB. We found that these extrinsic neurons innervate the lobes sequentially and their neurite arborizations in the MB lobe zones are independent of each other. Ablation of DAN axons or MBON dendrites in a zone had a minimal effect on other extrinsic neurites in the same or neighboring zones, suggesting that these neurons do not use tiling mechanisms to establish zonal borders. In contrast, KC axons are necessary for the development of extrinsic neurites. Dendrites of some vertical lobe-innervating MBONs were redirected to specific zones in the horizontal lobes when their normal target lobes were missing, indicating a hierarchical organization of guidance signals for the MBON dendrites. We show that Semaphorin 1a is required in MBONs to innervate three specific MB zones, and overexpression of *semaphorin 1a* is sufficient to redirect DAN dendrites to these zones. Our study provides an initial characterization of the cellular and molecular mechanisms underlying the assembly process of MB extrinsic neurons.

Drosophila | mushroom body | dopaminergic neurons | mushroom body output neurons | Semaphorin 1a

Significance

The adult *Drosophila* mushroom body (MB) is one of the most extensively studied neural circuits. However, how its circuit organization is established during development is unclear. In this study, we provide an initial characterization of the assembly process of the extrinsic neurons (dopaminergic neurons and MB output neurons) that target the vertical MB lobes. We probe the cellular mechanisms guiding the neurite targeting of these extrinsic neurons and demonstrate that Semaphorin 1a is required in several MB output neurons for their dendritic innervations to three specific MB lobe zones. Our study reveals several intriguing molecular and cellular principles governing assembly of the MB circuit.

The mushroom body (MB) is a computational center in the fly brain that controls diverse types of behavior, including learning and memory (1–5), sleep (6, 7), courtship (8–10), and foraging (11–14). MB functioning relies on its intricate circuit architecture that resembles the vertebrate cerebellum, being composed of a large number of parallel axonal fibers modularly innervated by afferent and efferent neurons (3, 15–18). The parallel axonal fibers of the MB are projected by ∼2,000 intrinsic Kenyon cells (KCs) in each brain hemisphere. These parallel fibers are bundled into five lobes, two of which extend vertically and are named the α and α′ lobes, and three that extend horizontally and are denoted the β, β′, and γ lobes (*SI Appendix*, Fig. S1*A*) (19). The primary afferent and efferent neurons of the MB lobes are the dopaminergic neurons (DANs) and MB output neurons (MBONs). A total of 21 types of DAN and 35 types of MBON have been identified (3, 18). Each type of DAN and MBON extends its axons or dendrites, respectively, into specific compartments or zones of the MB lobes. Together, DANs and MBONs subdivide the MB lobes into 15 distinct zones. Most DANs and MBONs innervate only one or two zones. Given that the MB lobes are bundles of continuous axonal processes, the way in which each type of DAN and MBON synapses with specific domains of the MB lobes represents an elaborate form of subcellular targeting. Similar but less elaborate subcellular neurite targeting has been documented in a variety of nervous systems (20–22). Uncovering the cellular and molecular mechanisms underlying the elaborate zonal organization of DAN and MBON neurites in the MB lobes should provide general insights into subcellular neurite targeting and complex neural circuit formation.

Our current understanding of MB development is mostly derived from studying the KCs. KCs are deposited by four neuroblasts in each brain hemisphere throughout the entirety of fly development (i.e., from embryonic to the end of the pupal stages) (23). These neuroblasts sequentially produce three major types of KCs, namely γ, α′β′, and αβ based on the lobes into which their axons extend (24). The larval MB mainly comprises γ and α′β′ KCs, whereas the adult MB has all three major KC types. The α′β′ and αβ KC axons have two branches, one projecting vertically to form the α′ and α lobes and the other extending horizontally to form the β′ and β lobes. The γ KC axons also have two branches at the larval stage. However, during early pupal development,

Author affiliations: [a]Department of Life Sciences and Institute of Genome Sciences, National Yang Ming Chiao Tung University, Taipei 112, Taiwan; [b]Institute of Molecular Biology, Academia Sinica, Taipei 115, Taiwan; [c]Taiwan International Graduate Program in Interdisciplinary Neuroscience, National Cheng Kung University and Academia Sinica, Tapiei 115, Taiwan; and [d]Taiwan International Graduate Program in Molecular and Cell Biology, Academia Sinica and Graduate Institute of Life Sciences, National Defense Medical Center, Taipei 115, Taiwan

Author contributions: C.-H.L., B.S., and S.L. designed research; C.-H.L., B.S., W.-J.C., and S.B. performed research; C.-H.L., B.S., and S.L. analyzed data; and C.-H.L. and S.L. wrote the paper.

The authors declare no competing interest.

This article is a PNAS Direct Submission.

[1]Present address: Centre for Neural Circuits and Behaviour, The University of Oxford, Oxford OX1 3SR, UK.

[2]To whom correspondence may be addressed. Email: sueweilin@gate.sinica.edu.tw.

This article contains supporting information online at http://www.pnas.org/lookup/suppl/doi:10.1073/pnas.2111283119/-/DCSupplemental.

Published March 14, 2022.

both branches are pruned, but only the horizontal branch is later regenerated and becomes a part of the adult MB (24).

In contrast to our knowledge of KC development, little is known about how the MBONs and DANs are incorporated into the MB circuit. Electron microscopy-based reconstructions of the first instar larval MB have revealed that even at this early developmental stage, the MB has already been extensively innervated by multiple extrinsic neurons, including seven types of DANs and 24 types of MBONs (25). These extrinsic neurons subdivide the first instar larval MB lobes into eight zones (plus two additional zones in the peduncle of the MB). This circuit architecture is maintained throughout larval development, with only a few other extrinsic neurons added when the larva grows from the first instar to the third instar stage (25, 26). During pupal development, the MB is remodeled, changing from two to five lobes, the DANs expand from seven to 21 types, and MBONs increase from 24 to 35 types (18, 25).

Although it is still unclear how neurites of these extrinsic neurons are zonally assembled into the MB circuit, a recent study showed that interactions between Dpr12 and DIP-δ play a critical role in zonal arborization of DAN axons projecting to the γ4 and γ5 zones in the γ lobe (27). DIP-δ-expressing DAN axons appear to innervate a zone at the distal end of the horizontal lobe during the late larval stage. These DAN axons stay at that position when the γ KC axons are pruned during early metamorphosis. When the γ KC axons regenerate, the DIP-δ-expressing DAN axons promote extension of the γ KC axons into the future γ4/5 zones. Meanwhile, DIP-δ induces clustering of Dpr12 in the γ KC axons at the γ4/5 zones, and Dpr12/DIP-δ interaction stabilizes the DAN axonal arbors within those zones. That study has provided the first clue as to how zonal innervation of DAN axons is refined and maintained during development. However, given that the γ lobe is the only MB lobe that undergoes remodeling during development, how the DAN axons establish their initial zonal innervation and whether the mechanisms that govern the assembly of extrinsic neurons into the γ lobe can be generalized to other lobes await investigation.

To gain further insights into assembly of the MB circuit, we investigated targeting of MBON dendrites and DAN axons to the MB vertical lobes (in particular to the α′ lobe) during the pupal stage when the adult MB circuit is being assembled. Our study focused on the vertical lobes because of their relative simplicity in terms of numbers and types of extrinsic neurons (3, 18). We followed the innervation process of vertical lobe-projecting DAN axons and MBON dendrites and performed genetic and chemical ablation experiments to probe the cellular mechanisms governing this process. We also identified Semaphorin 1a (Sema1a) as an important guidance molecule that controls zone-specific dendritic targeting for several MBONs (28). Our work provides an initial characterization of the cellular and molecular mechanisms underlying assembly of DANs and MBONs into the MB circuit.

Results

DAN Axons and MBON Dendrites Sequentially Innervate the MB Vertical Lobes. To investigate how the MB circuits are assembled, we first identified GAL4 lines in which individual types of DANs and MBONs projecting to the MB vertical lobes are labeled throughout their morphogenesis. Among all of the GAL4 lines we assessed (*SI Appendix*, Table S1), *MB058B-* and *MB091C-splitGAL4* specifically label PPL1-α′2α2 DANs and MBON-α′2, respectively, throughout their development (Fig. 1 *A–M* and *SI Appendix*, Fig. S1 *B–B′* and *F–F′*). Since PPL1-α′2α2 DANs and MBON-α′2 are the only DANs and MBONs that innervate the α′2 zone (3, 18), they provide an opportunity to study the innervation order of DAN axons and MBON dendrites in the same MB lobe zone, as well as their interactions with each other or with the neurons in neighboring zones.

First, we used *MB058B* and *MB091C* to drive expression of mCD8::GFP in PPL1-α′2α2 DANs and MBON-α′2 and checked their morphologies at various times after puparium formation (APF). The PPL1-α′2α2 DANs began to touch the MB lobes at 18 h APF, starting from the lateral surface of the α′ lobe near the position of the future α′2 zone (Fig. 1*A*). Since axons from a single PPL1-α′2α2 DAN innervate the MB vertical lobes in both hemispheres, we also generated single-cell flip-out clones (29) for PPL1-α′2α2 DANs and found that their ipsilateral and contralateral axonal innervations occurred simultaneously (*SI Appendix*, Fig. S2 *A–A′*). At 24 h APF, innervation in the α′2 zone became more obvious, with axons extending ventrally along the interfaces between the α′ and α lobes (Fig. 1*B* and *SI Appendix*, Fig. S2 *B* and *C*). Dense innervation in the α′2 zone was observed from 30 h APF onward (Fig. 1*C*), and innervation of the α2 zone at the middle segment of the α lobe began at 36 h APF (Fig. 1*D*). Dendritic targeting of MBON-α′2 to the α′2 zone occurred at a later time point. At 42 h APF, MBON-α′2 dendrites only began to innervate the medial surface of the α′2 zone (Fig. 1*K*), and more dense elaboration of the MBON-α′2 dendrites was seen at 48 h APF (Fig. 1*L*). Therefore, in the α′2 zone, DAN axons innervate the MB lobes earlier than MBON dendrites. This notion is further supported by colabeling experiments whereby PPL1-α′2α2 and MBON-α′2 were labeled simultaneously in distinct colors during pupal development (*SI Appendix*, Fig. S2 *D–E′*).

DAN axons do not always precede MBON dendrites in all MB lobe zones. In the α′3 zone, MBON dendrites appear to innervate the MB lobes earlier than the DAN axons. The α′3 zone is innervated by one PPL1-α′3 DAN (*SI Appendix*, Fig. S1 *E–E′*), two typical MBONs (MBON-α′3m and MBON-α′3ap; *SI Appendix*, Fig. S1 *C–C′*), and one atypical MBON-α′3 (MBON28) (18). By following the development of the two typical MBONs using *MB027B-splitGAL4* (Fig. 1 *N–S*), we revealed that their dendrites enter the MB lobe before 6 h APF. At this time point, the MBON-α′3m/ap dendrites concentrated at the center of the vertical lobe occupied by FasII-negative α′β′ KC axons, indicating that these dendrites have targeted the α′ lobe (Fig. 1 *R–R′*) (19). We have not identified GAL4 lines allowing us to follow the development of most other PPL1 DANs. However, when we labeled the DANs with antibodies against tyrosine hydroxylase (TH), an enzyme required for the synthesis of dopamine (30), we found that TH expression is sequentially turned on, beginning at the base of the vertical lobes and finishing at the tips of the α and α′ lobes (*SI Appendix*, Fig. S3). Expression of TH in the α′3 zone only became apparent at 48 h APF, representing the latest time point among all vertical compartments (*SI Appendix*, Fig. S3 *H–H′*). Anti-TH signal was first seen in the α′2 and α′1 zones at 24 h APF (*SI Appendix*, Fig. S3 *C–D′*), which matches the time when PPL1-α′2α2 and PPL1-γ2α′1 axons began to innervate these zones (Fig. 1 A–F and U–AA). These data support that TH staining can be used to report the innervation timings for PPL1 DANs and that MBON dendrites precede DAN axons in the α′3 zone. We acknowledge that TH expression may occur significantly later than axonal innervation in PPL1-α′3 and PPL1-α3 DANs. For instance, TH expression in DANs targeting the γ4/5 zones was shown to occur later than

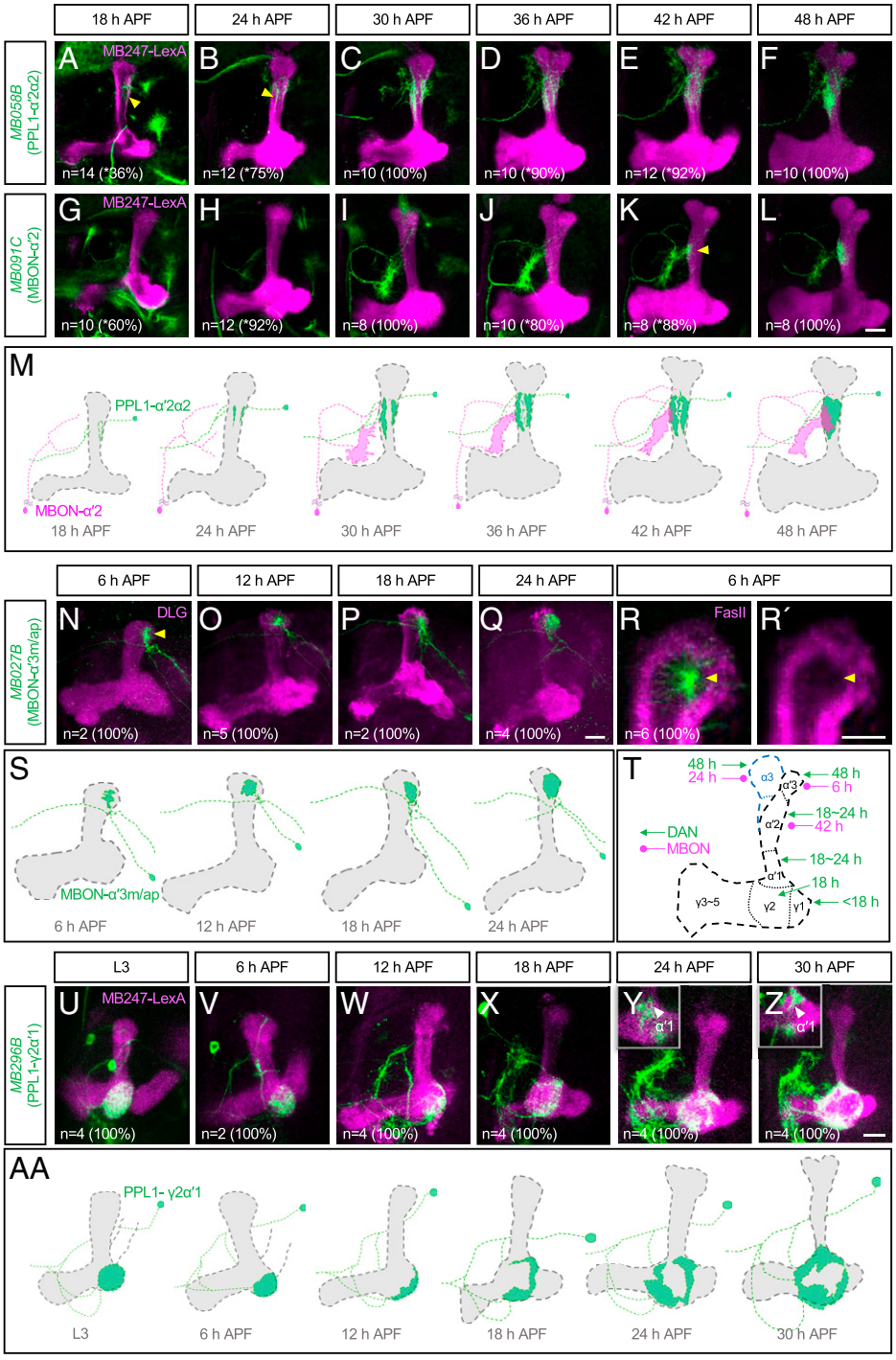

Fig. 1. Timing of innervations by DANs and MBONs targeting MB vertical lobes. (*A–F*) Axonal innervation in the MB vertical lobes by PPL1-α′2α2 DANs, labeled with *UAS-mCD8::GFP* driven by *MB058B-splitGAL4* (green), at different hours after puparium formation (APF). The yellow arrowheads in (*A*, *B*) indicate where the axons start to innervate the MB lobes. (*G–L*) Dendritic innervation in the MB vertical lobes by MBON-α′2, labeled by *MB091C-split-GAL4* driving *UAS-mCD8::GFP* (green), at different hours APF. The yellow arrowhead in (*K*) indicates where the dendrites start to innervate the MB lobes. MB lobes were labeled with *LexAop-rCD2::RFP* driven by *MB247-LexA::p65* (magenta) in (*A–L*). The n and (%) in this and following figures indicate the sample size and the percentage of the sample displaying the same phenotype as the representative image. *****Note that at 18 h APF, around half of the hemibrains did not contain PPL1-α′2α2 DANs (64%) or MBON-α′2 (40%). At 24 h APF, 25% of PPL1-α′2α2 DANs exhibited innervation patterns similar to that of 18 h APF, whereas 8% of MBON-α′2 showed innervation patterns similar to that of 30 h APF. At 36 h APF, 10% of PPL1-α′2α2 DANs exhibited innervation patterns similar to that of 42 h APF, whereas 20% of MBON-α′2 showed innervation patterns similar to that of 30 h APF. At 42 h APF, 8% of PPL1-α′2α2 DANs and 12% of MBON-α′2 exhibited innervation patterns similar to those of 48 h APF. (*M*) Schematics illustrating the timing of innervations for PPL1-α′2α2 axons (green) and MBON-α′2 dendrites (magenta) in the MB lobes. (*N–Q*) Dendritic targeting of MBON-α′3m/ap labeled with *UAS-mCD8::GFP* driven by *MB027B-splitGAL4* (green) at different hours APF. All KC axons were labeled with anti-DLG antibody (magenta). (*R–R′*) A magnified view of MBON-α′3m/ap dendritic innervation (green) in the MB vertical lobe labeled with anti-FasII antibody (magenta) at 6 h APF. A single focal plane is shown to demonstrate that the dendrites are concentrated at the FasII-negative core of the MB vertical lobe. (*S*) Schematics illustrating the results in (*N–Q*). (*T*) A summary of the innervation timings for DAN axons and MBON dendrites projecting to the indicated zones. The timings are based on data in Fig. 1 and *SI Appendix*, Fig. S3 and Table S1. (*U–Z*) Axonal innervations of PPL1-γ2α′1 labeled with *UAS-mCD8::GFP* driven by *MB296B-splitGAL4* (green) at different times during larval (third instar stage, L3) and pupal development. All KC axons were labeled with *LexAop-rCD2::RFP* driven by *MB247-LexA::p65* (magenta). *Insets* in (*Y*) and (*Z*) are single-focal-plane images showing the innervation of PPL1-γ2α′1 axons in the α′1 zone. Note that PPL1-γ2α′1 axons densely innervate the heel region of the L3 MB (*U*), and the axons are mostly pruned by 12 h APF (*W*). The pruned axons are re-extended to cover the γ2 zone from 18 h APF. Obvious axonal innervation in the α′1 zone can be observed at 24 h APF (*Y*). The innervation becomes very dense at 30 h APF, when the γ2 zone has not been fully covered by the axons (*Z*). (*AA*) Schematics illustrating the results in (*U–Z*). Scale bars, 15 μm.

their axonal innervation (27). Therefore, the precise timing for when these DAN axons innervate the vertical lobes remains to be confirmed. Nevertheless, our results strongly suggest that DAN axons and MBON dendrites sequentially innervate the MB vertical lobes, and their innervation order in a given zone may vary among zones (Fig. 1 *T*).

DANs and MBONs Independently Innervate MB Lobe Zones. Given that the axons of PPL1-α′2α2 DANs precede the MBON-α′2 dendrites in the α′2 zone, next we examined the possibility that DAN axons provide guidance cues for MBON dendrites in this zone. We genetically ablated PPL1-α′2α2 DANs by ectopically expressing the proapoptotic genes *head involution defective* (*hid*) and *reaper* (*rpr*) (31, 32) in these neurons using *MB058B-splitGAL4*. No *MB058B*-positive cells were seen in PPL1-α′2α2 DAN-ablated adult brains, and the α′2 and α2 zones lacked anti-TH staining signal (Fig. 2 *A–B′*). Ablation of PPL1-α′2α2 DANs occurred before 24 h APF (i.e., by the time PPL1-α′2α2 DANs start to innervate MB lobes in wild-type brains) (*SI Appendix*, Fig. S4 *A–F*). The TH-negative zones in the PPL1-α′2α2 DAN-ablated brains indicate that axon-axon contacts between neighboring DANs have a minimal effect in determining the borders of DAN axon zonal networks. To further confirm this notion, we labeled the PPL1 DANs

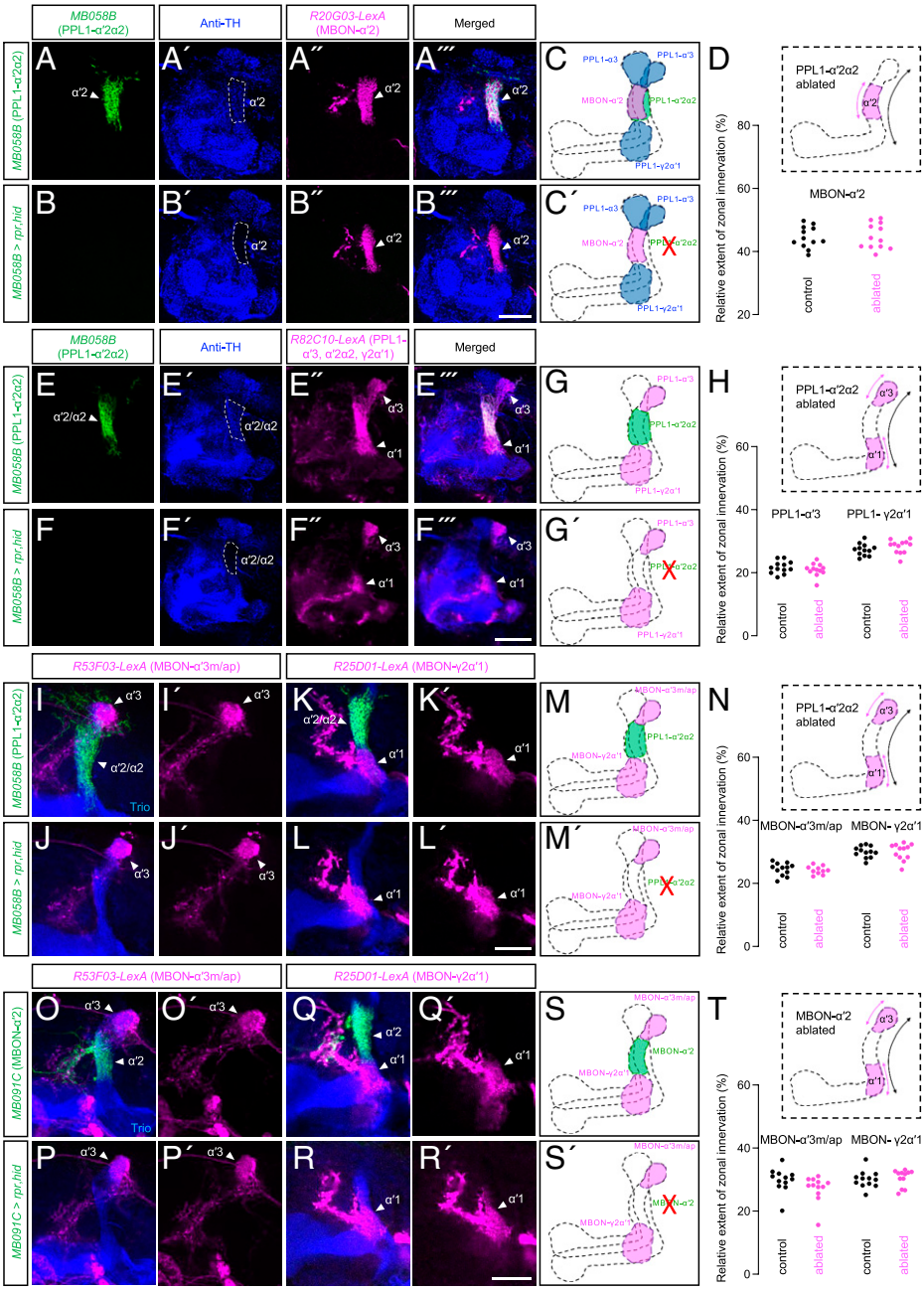

Fig. 2. Independent innervations by DANs and MBONs targeting the MB vertical lobes. (*A*–*A*‴) A wild-type brain whose PPL1-α′2α2 DANs were labeled with *UAS-mCD8::GFP* driven by *MB058B-splitGAL4* (green) and whose MBON-α′2 was labeled with *LexAop-rCD2::RFP* driven by *R20G03-LexA* (magenta). The brain was counterstained with anti-TH antibody to label DANs (blue). A single focal plane covering the α′2 zone is shown. (*B*–*B*‴) As for (*A*–*A*‴), except that PPL1-α′2α2 DANs were ablated with *UAS-rpr,hid* driven by *MB058B-splitGAL4*. (*C*–*C*′) Illustrative summary of the results in (*A*–*B*‴). (*D*) The relative extent of zonal innervation by MBON-α′2 dendrites was not affected by the ablation of PPL1-α′2α2 (two-tailed unpaired *t* test, $P = 0.8566$, $n = 12$). The extent of zonal innervation in this and following figures was measured by the distance between the midpoint of the upper border to the midpoint of the lower border of the neurite-covered area along the α′ lobe. The relative extent of zonal innervation was calculated as [(extent of dendritic or axonal innervation ÷ length of the α′ lobe from the tip to the bifurcation point) × 100]. (*E*–*H*) Same as (*A*–*D*), except that *R82C10-LexA* was used to label PPL1-α′3, -α′2α2, and -γ2α′1 DANs (magenta) (two-tailed unpaired *t* test, PPL1-α′3: $P = 0.3534$, PPL1-γ2α′1: $P = 0.2471$, $n = 12$). (*I*–*N*) Same as (*A*–*D*), except that the tested neurons were MBON-α′3m/ap and MBON-γ2α′1 labeled by *R53F03-LexA* and *R25D01-LexA*, respectively. The brains were counterstained with anti-Trio antibody to label α′β′ and γ lobes (blue) (two-tailed unpaired *t* test, MBON-α′3m/ap: $P = 0.7021$, MBON-γ2α′1: $P = 0.9685$, $n = 10$–12). (*O*–*T*) Same as (*I*–*N*), except that the neuron being ablated is MBON-α′2 labeled by *MB091C-splitGAL4* (green) (two-tailed unpaired *t* test, MBON-α′3m/ap: $P = 0.1187$, MBON-γ2α′1: $P = 0.6925$, $n = 12$). Scale bars, 25 μm.

innervating the α′ lobe with *R82C10-LexA* and found that the PPL1-α′3 and PPL1-γ2α′1 neurites were confined to their original area (Fig. 2 *E*–*G*′ and *SI Appendix*, Fig. S1 *D*–*E*′). We then measured the extents of zonal innervation by PPL1-α′3 and PPL1-γ2α′1 in the α′ lobe. No difference was detected between the normal and PPL1-α′2α2-ablated MB (Fig. 2*H*), so zonal innervation of the neighboring DAN axons is not affected by loss of PPL1-α′2α2. Ablation of PPL1-α′2α2 DANs also did not affect dendritic targeting of MBON-α′2, indicating that PPL1-α′2α2 DANs do not provide guidance cues for MBON-α′2 dendrites (Fig. 2 *A*′′–*D*). Moreover, ablation of PPL1-α′2α2 DANs had no effect on the dendritic elaboration of typical α′3-projecting MBONs (MBON-α′3m/ap) or MBON-γ2α′1 in the neighboring zones (Fig. 2 *I*–*N*).

Next, we tested if interaction between MBON dendrites in the neighboring zones is required to establish zonal borders. Ablation of MBON-α′2 before its dendrites innervate the MB lobes did not influence zonal elaboration of MBON-α′3m/ap or MBON-γ2α′1 dendrites (Fig. 2 *O–T* and *SI Appendix*, Fig. S4 *G–L*). These dendrites were still confined to their normal position, and their coverage along the α′ lobe remained unchanged. Similarly, MBON-α′2 dendrites were also unaffected when MBON-α′3m/ap was ablated early in development (*SI Appendix*, Figs. S4 M–O and S5 *A–C*). These results support that dendritic tiling (33, 34) is not the mechanism by which the borders between MBON dendrites in neighboring zones are determined, at least for the neurons and zones that we have examined. We note that *MB027B-splitGAL4*, which we used to manipulate and visualize MBON-α′3m/ap, does not label the recently identified atypical MBON-α′3 (18). Given that dendrites of atypical MBONs only partially innervate the MB lobes, whether our observations for typical MBONs can be applied to atypical MBONs remains to be determined. Furthermore, although ablating PPL1-α′2α2 or MBON-α′2 individually does not affect neurite innervations in the neighboring zones, we were not able to precisely ablate both neuron types due to nonspecific labeling of background neurons when *MB058-* and *MB091C-splitGAL4* were combined. Therefore, it is unclear how ablation of both MBONs and DANs in a given zone affects the neighboring neurites.

MBON-α′2 likely does not guide the innervation of PPL1-α′2α2 axons since MBON-α′2 dendrites arrive at the α′ lobe after PPL1-α′2α2 axons have already established zonal arborization. However, when we labeled PPL1 DANs with *R82C10-LexA* and measured their neurite density in the α′2 and α2 zones of the adult MB, we found that neurite density in the α′2 zone was reduced upon MBON-α′2 ablation (*SI Appendix*, Fig. S5 *D–F*). A similar reduction was observed when we specifically labeled PPL1-α′2α2 DANs by creating single-cell flip-out clones (*SI Appendix*, Fig. S5 *G–I*). In contrast, the extent of zonal innervation for PPL1-α′2α2 axons in the α′2 zone was not affected by MBON-α′2 ablation (*SI Appendix*, Fig. S5*I*′), nor was innervation of the neighboring PPL1-α′3 and -γ2α′1 axons (*SI Appendix*, Fig. S5 *J–O*). Therefore, although MBON-α′2 is not required for zonal targeting of PPL1-α′2α2 axons, their synaptic connections may be important for maintaining the proper density of PPL1-α′2α2 axonal arbors. Taken together, these findings suggest that zonal elaborations of DAN axons and MBON dendrites in the MB vertical lobes are largely independent of each other.

MB Lobes Are Essential for Zonal Elaborations of DAN Axons. Since the zonal targeting of DANs and MBONs is not governed by their mutual interactions, next we investigated the role of MB lobes in this process using the *alpha lobe absent* (*ala*) fly mutant. Brains of the *ala* mutant randomly lose vertical or horizontal lobes of the MB (35, 36). The main framework of the MB lobes are formed by KC axons, and in *ala* mutants lacking vertical MB lobes, around half of the α′β′ and αβ KCs lose their vertical branches and the vertical branches of the remaining half project horizontally (35). We found that when MB vertical lobes on one side of the brain were absent, both contralateral and ipsilateral PPL1-α′2α2 axons extended to areas near their missing targets without forming normal zonal elaboration patterns (Fig. 3 *A–B*′). Mistargeting of PPL1-α′2α2 axons was completely correlated with the lobe-absent phenotype ($n = 14$), so it was not caused by loss of the *ala* gene per se but due to lack of vertical lobes.

We also examined PPL1-α′2α2 axons in the *ala* mutant brains at 30 h APF, when obvious zonal innervation by the axons is first observed. We found that when vertical lobes were absent, PPL1-α′2α2 axons failed to form a zonal network from the very beginning of the elaboration process, and some mistargeted neurites could be found above and posterior to where the α′2 and α2 zones are supposed to be located (*SI Appendix*, Fig. S6 *A–C*′). A similar misrouting phenotype was observed for the axons of PPL1-α′3 DANs (*SI Appendix*, Fig. S6 *D–F*). Since these mistargeted axons could still project to sites close to their normal targets, the MB lobes do not appear to provide long-range guidance cues for these axons. Instead, the MB lobes may provide local positional cues for the DAN axons to form zonal networks. This latter scenario was further evidenced when we used a multicolor flip-out technique (29) to label PPL1-α′2α2 and PPL1-α′3 DANs in different colors in the same brain (*SI Appendix*, Fig. S6 *K–K*″). We found that the primary neurites of these two DANs entered the MB lobes at a similar location. However, PPL1-α′2α2 axons exclusively occupied the α′2 and α2 zones below the entry point, whereas PPL1-α′3 axons specifically covered the α′3 zone above the entry point, suggesting local cues exist that direct zonal elaboration of DAN axons.

MBON-α′2 Dendrites Respond to Distinct Signals from Different MB Lobe Zones. Surprisingly, when the MB vertical lobes were absent, we observed misguided MBON-α′2 neurites innervating other lobe regions resembling the β′2 and α′1 zones (Fig. 3*C*). We confirmed that these ectopic neurites are dendrites by labeling MBON-α′2 with the dendritic marker DenMark (37) and axonal marker DSyd-1-GFP (38) (*SI Appendix*, Fig. S7 *A–A*″). When we followed the development of the MBON-α′2 dendrites in the absence of their normal target, we found that they never formed a zonal network near the missing target, but started to innervate the β′2- and α′1-like zones at ∼72 h APF (*SI Appendix*, Fig. S7 *B–D*′). As mentioned previously, approximately half of the α′β′ and αβ KCs exhibit two horizontal-projecting axonal branches in vertical lobe-absent *ala* MBs (35). Although it is unclear if the additional horizontal-projecting branches retain their original identity or adopt characteristics of the horizontal branch, is it possible that the MBON-α′2 dendrites followed the α′2 zone in the now "collapsed" vertical lobes? We argue that this is an unlikely scenario because the zones innervated by the mistargeted MBON-α′2 dendrites are located at either end, but not in the middle, of the horizontal lobes. Furthermore, we have performed GFP reconstitution across synaptic partners (GRASP) (39), in which one split-GFP fragment (GFP1-10) was expressed in MBON-α′2, while the complementary GFP fragment (GFP11) was expressed in *R48B04-LexA*-labeled DANs in the protocerebral anterior medial (PAM) cluster projecting to β′2 and γ5 zones in the MB horizontal lobes (40). GRASP signals in the β′2 zone, which imply putative synaptic connections between MBON-α′2 and β′2-projecting DANs, were detected only in *ala* brains where MBON-α′2 dendrites were mistargeted (Fig. 3 *F* and *G*). Since axonal innervation of the β′2-projecting PAM-DANs is unaffected in the vertical lobe-absent *ala* MB (*SI Appendix*, Fig. S6 *I–J*′), these results support that MBON-α′2 dendrites can be rerouted to the β′2 zone and form putative synaptic connections with local DAN axons when the normal target of MBON-α′2 is absent. Not all vertical lobe-projecting MBON dendrites were redirected to other zones when the MB vertical lobes were missing. For example, MBON-α′3m/ap dendrites densely innervate the α′3 zone in the wildtype brain (*SI Appendix*, Fig. S6*G*), and loss of MB vertical lobes resulted in

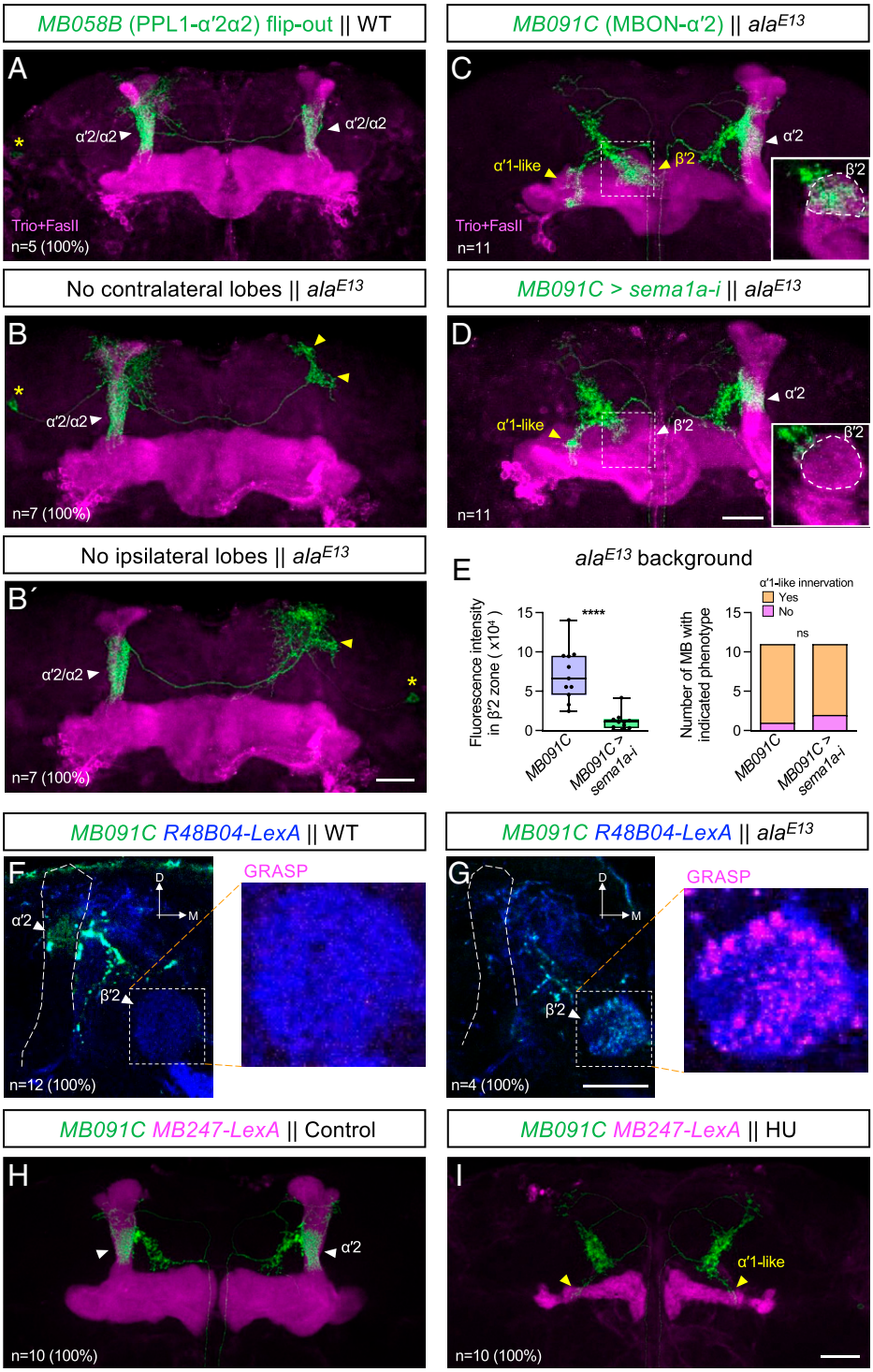

Fig. 3. Loss of MB vertical lobes results in mistargeted PPL1-α′2α2 axons and MBON-α′2 dendrites. (*A*–*B*′) Single-cell multicolor flip-out clones of PPL1-α′2α2 DANs (green) in wild-type (WT; *A*) and *ala*^{E13} (*B*–*B*′) brains from which the MB has lost its vertical lobes on the contralateral (*B*) or ipsilateral (*B*′) side to the clones, whose cell bodies are marked by asterisks. The yellow arrowheads indicate the misguided neurites near their missing targets. The brains were counterstained with anti-Trio and anti-FasII antibodies to label all MB lobes (magenta). (*C*) Innervation pattern of MBON-α′2 dendrites labeled with *UAS-mCD8::GFP* driven by *MB091C-splitGAL4* (green) in an *ala*^{E13} brain in which the vertical lobes are missing in one hemibrain. The yellow arrowheads indicate the mistargeted dendrites in the β′2 and α′1-like zones. (*D*) As for (*C*), but *sema1a* was additionally knocked down in MBON-α′2. *Insets* in (*C*, *D*) are single-focal plane images of the β′2 zone. (*E*) Innervations of MBON-α′2 dendrites, indicated as green fluorescence intensity, in the β′2 zone are significantly different between control (*MB091C* only) and *sema1a* knockdown (*MB091C* > *UAS-sema1a-i*) brains (two-tailed unpaired *t* test, $P < 0.0001$, $n = 11$). Innervations of MBON-α′2 dendrites in the α′1-like zone are not different between control and *sema1a* knockdown brains (Fisher's exact test, $P > 0.9999$, $n = 11$). (*F*, *G*) GRASP signals (magenta) indicating synaptic reconstitution of GFP1-10 and GFP11 expressed in MBON-α′2 (by *MB091C-splitGAL4*) and PAM-DANs (by *R48B04-LexA*), respectively, were only detected in the *ala* brains where MBON-α′2 dendrites were mistargeted to the tip of the β′ lobe. (*H*, *I*) Innervation patterns of MBON-α′2 dendrites labeled with *UAS-mCD8::GFP* driven by *MB091C-splitGAL4* (green) in the control (*H*) and HU-ablated (*I*) MBs. The yellow arrowheads in (*I*) indicate the misguided neurites extending toward the putative positions of α′1-like zone. Scale bars, 25 μm.

sparse arborization of these dendrites in areas posterior to their missing target (*SI Appendix*, Fig. S6*H*).

To examine if the horizontal lobes can potentially provide guidance to the misrouted MBON-α′2 dendrites in the *ala* brain, we ablated all but a few embryonic-born KCs by feeding newly hatched larvae 50 mg/mL hydroxyurea (HU) for 4 h (1, 41). This treatment ablated all α′β′, αβ, and most γ KCs, so only a slender γ lobe was observed in the respective adult MB (Fig. 3 *H* and *I*). Under this condition, no MBON-α′2 neurite was found in either the β′2 or α′2 zone, indicating that the β′ lobe is critical for zonal innervation of MBON-α′2 dendrites in the β′2 zone. Interestingly, when we ablated the MB by means of HU treatment, MBON-α′2 still extended ectopic neurites toward the position of the α′1-like zone, but did not form zonal arborization there. Hence, long-distance orientation of these neurites is likely directed by other cells, whereas their zonal innervation is promoted by the MB lobes. Taken together, our data indicate that MB lobes play an important role in guiding the innervation of MBON dendrites, and MBON-α′2 dendrites can respond to diverse guidance cues that direct them to different MB lobe zones.

To gain insights into the guiding mechanisms that direct the MBON-α′2 dendrites to different MB lobe zones, we searched for molecules whose expression in MBON-α′2 affect its dendritic targeting. Sema1a is a transmembrane protein that has been shown to mediate both axonal and dendritic guidance (42–46). Therefore, we tested if Sema1a may play a role in guiding MBON-α′2 dendrites. Interestingly, when we knocked down *sema1a* in MBON-α′2, although its normal dendritic innervation in the α′2 zone was unaffected (*SI Appendix*, Fig. S7 *E* and *F*), its dendritic mistargeting in the β′2 zone of *ala* mutant brains was disrupted (Fig. 3 *D* and *E*). The efficiency of the *sema1a* RNAi line, *UAS-sema1a-RNAi*^{HMS01307}, that we used in the knockdown experiments has been demonstrated previously (47). To assess if MBON-α′2 expresses *sema1a*, we used a genetically modified *sema1a*^{FSF} allele that allows conditional V5-tagging of endogenous Sema1a in neurons expressing flippase (FLP) (*SI Appendix*, Fig. S8 *O–O′*) (48). Using *MB091C* to drive FLP in MBON-α′2, we observed clear expression of V5-tagged Sema1a in these neurons during early pupal stages (*SI Appendix*, Fig. S8 *A–C′*). In contrast to *sema1a*-dependent rerouting of the β′2-projecting dendrites, *sema1a* is dispensable for MBON-α′2 dendrites to innervate the α′1-like zone (Fig. 3 *D* and *E*). Taken together, these experiments show that distinct MB lobe zones use *sema1a*-dependent and -independent mechanisms to guide the MBON-α′2 dendrites.

Sema1a Is Required for Dendritic Targeting of β′2-Innervating MBONs. Since MBON-α′2 dendrites used a *sema1a*-dependent mechanism to innervate the β′2 zone of *ala* mutant brains, we reasoned that *sema1a* may also play a role in MBON dendrites that normally target to this zone. The β′2 zone can be further subdivided into anterior (a), medial (m), and posterior (p) regions, which are innervated by the dendrites from several MBON types, including MBON-γ5β′2a, MBON-β2β′2a, and MBON-β′2mp (*SI Appendix*, Fig. S1 *G–I″*) (3, 18). Consistently, RNA interference (RNAi) knockdown of *sema1a* in MBON-β2β′2a using *MB399C-splitGAL4* resulted in mistargeting of the dendrites that normally innervate the β′2a zone. Instead of innervating the β′2a zone, these dendrites projected upwards to regions near the central complex (Fig. 4 *A* and *B* and *SI Appendix*, Fig. S9 *A* and *B*). The MBON-β2β′2a dendrites innervating the β2 zone were less affected by *sema1a* knockdown, suggesting that *sema1a* regulates dendritic targeting of MBON-β2β′2a in a zone-specific manner.

To confirm the specificity of RNAi knockdown, we overexpressed full-length *sema1a* (42) together with *sema1a* RNAi in MBON-β2β′2a. The *sema1a* RNAi targets the 5′-UTR of the *sema1a* transcript and thus will not affect the overexpressed *sema1a* that contains only the coding sequence (49). Overexpression of *sema1a* proved sufficient to rescue the dendritic mistargeting phenotype (Fig. 4*C*), supporting that the phenotype specifically arose from *sema1a* knockdown. Sema1a functions as a ligand or receptor in a context-dependent manner. When functioning as a ligand, Sema1a binds to receptors in the receiving cells to activate canonical "forward signaling" (45, 50). In contrast, when serving as a receptor, Sema1a is activated by membrane-bound or secreted ligands, and its cytoplasmic domains are required to transduce reverse signaling via the Rho family small GTPase Pebble and RhoGAPp190 (42, 51, 52). To test if the intracellular domain of Sema1a is important for guidance of MBON-β2β′2a dendrites, we overexpressed Sema1a lacking the intracellular domain [Sema1a.mEC-myc and Sema1a.mEC.Fc-myc (42)] and found that they failed to rescue the RNAi-induced dendritic mistargeting phenotype (Fig. 4 *D–G*). These results indicate that Sema1a functions as a receptor in MBON-β2β′2a to direct their dendrites to the β′2a zone.

We have not identified GAL4 lines that are expressed during early development of MBON-β′2mp and MBON-γ5β′2a. Therefore, we tested the role of *sema1a* in these neurons using mosaic analysis with a repressible cell marker (MARCM), a genetic method for generating homozygous mutant cells in a heterozygous mutant background (53). Similar to our observations for MBON-β2β′2a, *sema1a*^{k13702} MARCM clones for MBON-γ5β′2a lost their dendritic innervation in the β′2a zone and had misguided neurites around the distal part of the horizontal MB lobes (*SI Appendix*, Fig. S9 *C–D′*). Their dendritic innervation to the γ5 zone was unaffected. The *sema1a* ^{k13702} MARCM clones for MBON-β′2mp labeled with DenMark and DSyd-1-GFP also exhibited dendritic targeting defects. In these mutant clones, dendritic innervation in the β′2mp zone became sparser, and ectopic neurites were observed around the zone (Fig. 4 *H–K″*). Taken together, these results indicate that *sema1a* is required for the dendritic targeting of MBONs to the β′2 zone.

Next, we examined *sema1a* expression in MBON-β2β′2a and MBON-β′2mp using the *sema1a*^{FSF} allele. V5-tagged Sema1a was observed in both MBON-β2β′2a and MBON-β′2mp at early pupal stages, indicating that these neurons express *sema1a* endogenously (*SI Appendix*, Fig. S8 *D–I′*). However, Sema1a appeared to be uniformly distributed in the neurites of these MBONs. Therefore, the differential effect of *sema1a* knockdown on the MBON-β2β′2a dendrites projecting to the β′2a and β2 zones cannot be explained by Sema1a distribution (*SI Appendix*, Fig. S8 *D–F′*). Instead, the guidance cues that attract Sema1a-positive dendrites may mainly be present in the β′2a zone. We could not examine expression of *sema1a* in MBON-γ5β′2a during development because GAL4 lines to drive FLP expression sufficiently early are currently not available. However, when we drove FLP expression with *MB210B-splitGAL4* and examined the adult brains, V5-tagged Sema1a was also observed in MBON-γ5β′2a (*SI Appendix*, Fig. S8 *M* and *N*).

Overexpression of _sema1a_ in DANs Drives Their Dendrites to Specific MB Lobe Zones. Next, we tested if overexpression of *sema1a* can direct dendrites that normally do not innervate the β′2 zone to that zone. In all the brains we have examined, when *sema1a* was overexpressed in PPL1-α′2α2 DANs, some of

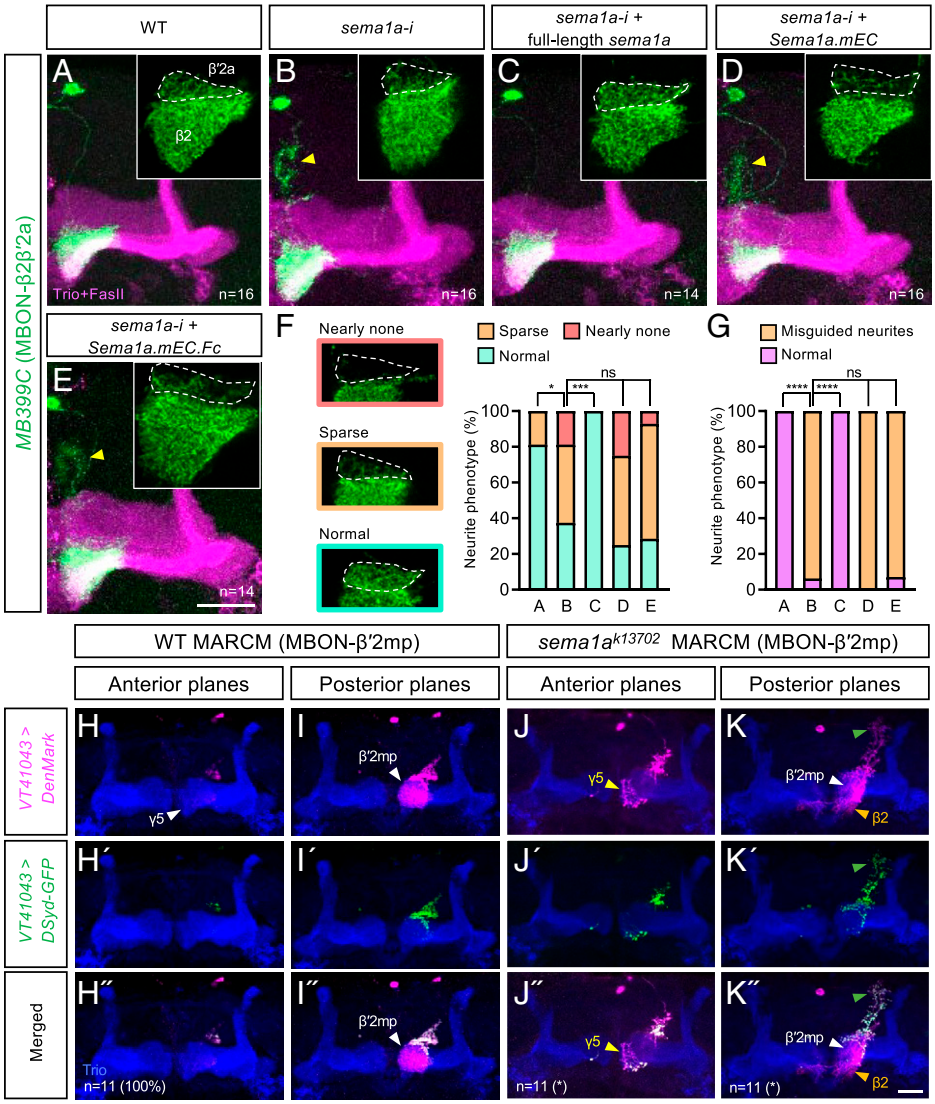

Fig. 4. Sema1a is required for MBON dendrites to innervate the β′2 zone. (*A*, *B*) Wild-type (*A*) and *sema1a* knockdown (*B*) MBON-β2β′2a labeled with *UAS-mCD8::GFP* driven by *MB399C-splitGAL4* (green). The yellow arrowhead in (*B*) indicates the misguided dorsally-projecting neurites. (*C*–*E*) Full-length Sema1a (*C*) or Sema1a lacking its intracellular domain (*D*, *E*) was coexpressed with *sema1a* RNAi in MBON-β2β′2a (green). All brains were counterstained with anti-Trio and anti-FasII antibodies to label all MB lobes (magenta). The *Insets* show single focal planes covering the β′2a (outlined by white dashed lines) and β2 zones. The yellow arrowheads in (*D*) and (*E*) indicate the misguided dorsally-projecting neurites. (*F*) Full-length Sema1a but not that lacking its intracellular domain rescues the neurite innervation defects in the β′2a zone caused by *sema1a* knockdown (Fisher's exact test, $*P < 0.05$, $***P < 0.001$, ns: $P > 0.7$, $n = 14$–16). Representative images for the three neurite innervation categories are shown on the left. (*G*) Full-length Sema1a but not that lacking its intracellular domain rescues the misguided neurite phenotype caused by *sema1a* knockdown (Fisher's exact test, $****P < 0.0001$, ns: $P > 0.9999$, $n = 14$–16). The letters below the bars in (*F*, *G*) correspond to panels A-E. (*H*–*K*″) Wildtype (*H*–*I*″) and *sema1a*^{k13702} (*J*–*K*″) MARCM clones for MBON-β′2mp labeled with *UAS-DenMark* (magenta) and *UAS-DSyd-1-GFP* (DSyd-GFP; green) driven by *VT41043-GAL4*. Brains were counterstained with anti-Trio antibody to label α′, β′, and γ lobes (blue). *****Eleven wild-type and 11 *sema1a*^{k13702} clones were imaged. All wild-type clones show normal β′2mp innervations (*H*–*I*″), and all *sema1a*^{k13702} clones exhibit loose or no β′2mp dendritic innervation (as indicated by white arrowheads; *K* and *K*″). Furthermore, of the 11 *sema1a*^{k13702} clones, 4 show ectopic dendritic innervations in the γ5 zone (as indicated by yellow arrowheads; *J* and *J*″), 3 show ectopic dendritic innervations in the β2 zone (as indicated by orange arrowheads; *K* and *K*″), and 7 show misguided neurites labeled by both DenMark and DSyd-1-GFP (as indicated by green arrowheads; *K*–*K*″). Scale bars, 25 μm.

their dendrites that normally arborize in brain areas posterior to the MB vertical lobes were rerouted to the β′2 zone, mostly in the posterior domain (i.e., β′2p zone) (Fig. 5 *A* and *B*). Intriguingly, *sema1a* overexpression also sent some PPL1-α′2α2 dendrites to α′1 and α′3 zones, suggesting that these zones also have the ability to attract *sema1a*-positive dendrites. We confirmed that these misguided neurites are dendrites by labeling PPL1-α′2α2 with DenMark and DSyd-1-GFP (Fig. 5 *E*–*H*). Consistent with Sema1a functioning as a receptor in MBON-β2β′2a, overexpression of Sema1a lacking its intracellular domain in PPL1-α′2α2 DANs had no effect on their dendrites (Fig. 5 *C* and *D*).

To test if the redirected PPL1-α′2α2 dendrites caused by *sema1a* overexpression form synapses with KC axons, we performed functional GRASP (54), in which synaptobrevin-fused GFP1-10 (Syb::GFP1-10) was expressed in all KCs, and the complementary CD4::GFP11 was expressed in PPL1-α′2α2 together with *UAS-sema1a*. Synaptic GRASP signals were detected in the β′2, α′1, and α′3 zones (*SI Appendix*, Fig. S10 *A*–*B*′). Strong GRASP signals were also observed in the α′2/α2 zones, which is consistent with functional studies and electron microscopy-based connectome data showing the existence of KC-to-DAN synapses in the MB lobes (18, 55, 56). Therefore, overexpression of *sema1a* in PPL1-α′2α2 neurons appears to reconfigure the MB circuit by misconnecting PPL1-α′2α2 dendrites to the KC axons.

Overexpression of *sema1a* in PPL1-γ2α′1 DANs using *MB296B-splitGAL4* also caused mistargeted dendrites, but they

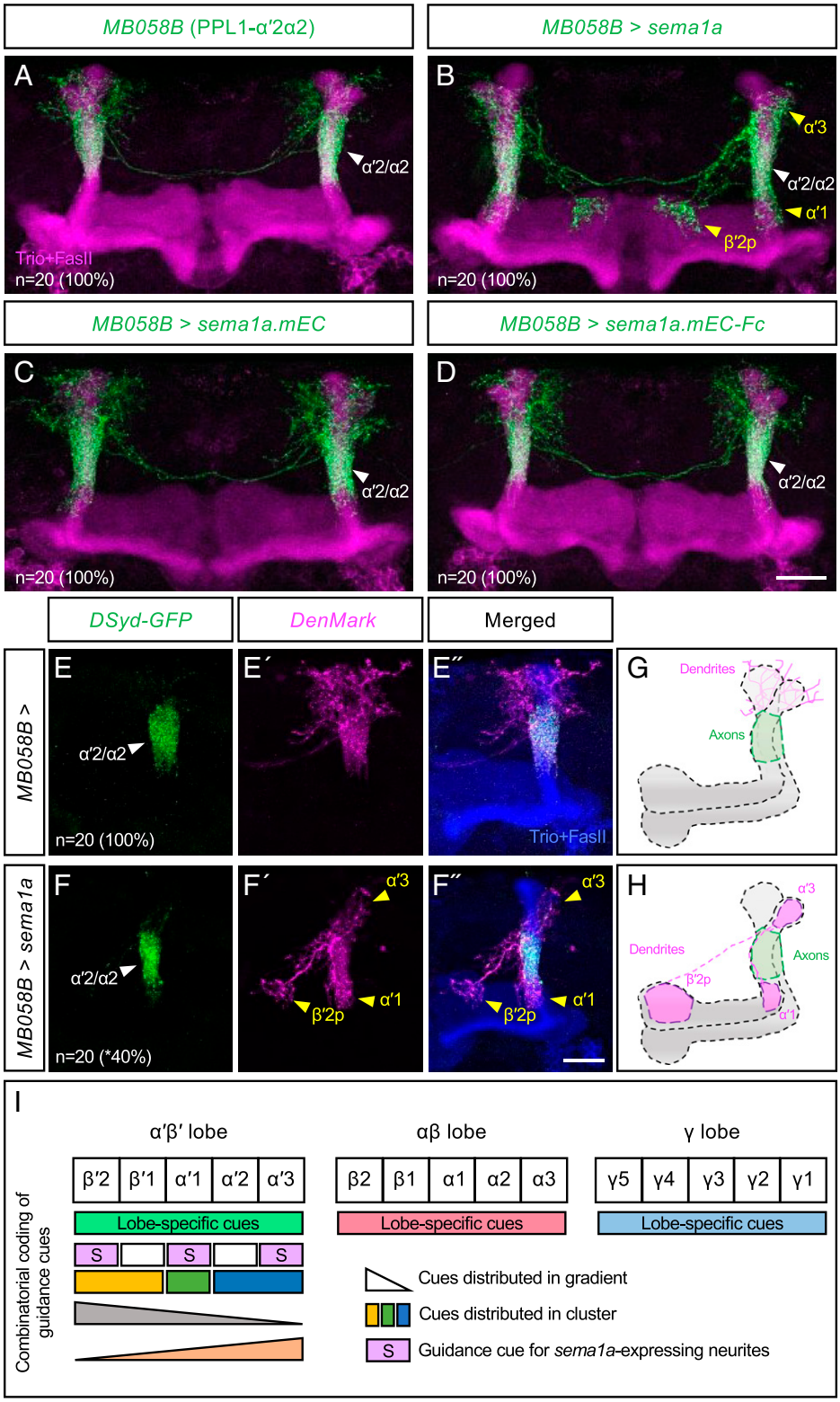

Fig. 5. Overexpression of *sema1a* redirects PPL1-α′2α2 dendrites to specific MB lobe zones. (*A*–*D*) Wildtype PPL1-α′2α2 DANs (*A*) and PPL1-α′2α2 DANs overexpressing normal Sema1a (*B*) or Sema1a lacking the intracellular domain (*C*, *D*). PPL1-α′2α2 DANs were labeled with *UAS-mCD8::GFP* driven by *MB058B-splitGAL4* (green). Brains were counterstained with anti-Trio and anti-FasII antibodies to label all MB lobes (magenta). The yellow arrowheads in (*B*) indicate the misguided dendrites in three MB lobe zones. (*E*–*F*′′) Wildtype (*E*–*E*′′) and *sema1a*-overexpressing (*F*–*F*′′) PPL1-α′2α2 DANs labeled with *UAS-DSyd-1-GFP* (DSyd-GFP; green) and *UAS-DenMark* (magenta) driven by *MB058B-splitGAL4*. Brains were counterstained with anti-Trio and anti-FasII antibodies to label all MB lobes (blue). The yellow arrowheads in (*F*′) and (*F*′′) indicate the misguided dendrites in three MB lobe zones. *****Note that although all the brains examined had DenMark signals in the α′1 and α′3 zones, only 40% of them showed DenMark signals in the β′2 zone. This outcome could be due to insufficient transportation of the DenMark proteins or expression of *sema1a* was lower in the presence of too many *UAS*-transgenes. Alternatively, some of those β′2-projection dendrites might be immature. (*G*, *H*) Illustrative summaries of the results in (*E*–*F*′′). Scale bars, 25 μm. (*I*) A conceptual model for how the positional cues in the MB lobes might be hierarchically organized and work in combination to guide the zonal innervations by MBON dendrites and DAN axons. Broadly expressed lobe-specific cues provide general attraction for MBONs innervating each of the three major lobe types. Zone-specific guidance is then instructed by combinations of diverse guidance cues, which can be clustered at specific zones or distributed as concentration gradients along the lobes.

innervated all three domains of the β′2 zones (i.e., β′2m, β′2p, and β′2a zones) (*SI Appendix*, Fig. S10 *C–E′*). Therefore, overexpression of *sema1a* in different DANs targets their dendrites to distinct domains of the β′2 zones. These results indicate that Sema1a may work with other guidance molecules to refine innervating regions for different dendrites. Overexpression of *sema1a* cannot always outcompete the endogenous dendritic targeting program, as is evident for MBON-α′2 in which overexpression of *sema1a* did not lead to dendritic retargeting to the β′2, α′1, or α′3 zones (*SI Appendix*, Fig. S7*G*).

The ectopic innervation of *sema1a*-overexpressed PPL1-α′2α2 in the α′1 and α′3 zones prompted us to examine the role of *sema1a* in dendritic targeting of the MBONs normally innervating these zones. The α′3 zone is innervated by MBON-α′3m/ap dendrites, and when *sema1a* activity was removed from MBON-α′3m/ap, its dendrites failed to concentrate in the α′3 zone but instead arborized sparsely around the vertical MB lobes (*SI Appendix*, Fig. S9 *E* and *F*). Moreover, endogenously-expressed Sema1a-V5 was detected in MBON-α′3m/ap during development (*SI Appendix*, Fig. S8 *J–L′*). Therefore, *sema1a* is required cell autonomously for the dendritic targeting of MBON-α′3m/ap.

The α′1 zone is innervated by dendrites from several MBONs, including MBON-α′1 (or MBON15) and MBON-γ2α′1 (3, 18). Dendritic innervation in the α′1 zone was unaffected in $sema1a^{k13702}$ MARCM clones for MBON-γ2α′1 (*SI Appendix*, Fig. S9 *I* and *J*). In contrast, $sema1a^{k13702}$ MARCM clones for MBON-α′1 exhibited a severe dendritic targeting defect. We induced clones at 4–8 h after egg laying (AEL) and labeled the MBON-α′1 dendrites using *R24H08-GAL4*, which also labels MBON-α′3m/ap dendrites. In wild-type clones, MBON-α′1 dendrites were always accompanied by those of MBON-α′3m/ap, suggesting that these two neuron types are from the same neuronal lineage (*SI Appendix*, Fig. S9*G*). In $sema1a^{k13702}$ mutant clones, we identified the mistargeted MBON-α′3m/ap based on its residual dendritic innervation in the α′3 zone. However, in these clones ($n = 23$), we observed no (78%) or sparse (22%) neurite innervation in the α′1 zone (*SI Appendix*, Fig. S9*H*). The *R24H08*-labeled wildtype MBON-α′3m/ap/α′1 clones mostly had five cells (*SI Appendix*, Fig. S9*K*). There were fewer cells in the $sema1a^{k13702}$ clones, but in some of those containing five cells, we still did not observe innervation in the α′1 zone. These results support that dendritic targeting of MBON-α′1 is *sema1a*-dependent and that MBON-α′1 might die during development if its dendrites fail to find the correct presynaptic partners. Taken together, these experiments show that *sema1a* is necessary for most MBONs to target their dendrites to three specific zones of the MB lobes (β′2, α′1, and α′3), and that overexpression of *sema1a* in some DANs is sufficient to direct their dendrites to these zones.

Discussion

The MB is one of the most intensively studied structures in the fly brain. Its complex and organized circuit architecture has provided important clues to its operational logic (3, 4). However, in contrast to the extensive investigations of its functions, how the MB circuit architecture is established during development has been little explored. In this study, we provide an initial characterization of MB circuit assembly and identify Sema1a as an important guidance molecule that directs dendritic innervations of multiple MBONs in three MB lobe zones. Below, we discuss several implications of our study relating to the wiring principles of the MB circuit and propose a hypothetical model for how DAN axons and MBON dendrites are modularly assembled into the MB lobes.

The Independence of DANs and MBONs. The most intriguing feature of the organization of the MB circuit is the zonal innervation of the MB lobes by DAN axons and MBON dendrites. The borders of the zones are distinct, with minimal overlap between DAN axons or MBON dendrites in the neighboring zones. Given such a highly organized neural network, elaborate interactions among the extrinsic neurons might be expected. For example, dendritic tiling, as observed between dendritic arborization (da) neurons in fly larvae, might be required for the formation of zonal borders between MBON dendrites (34), and match-ups between DAN axons and MBON dendrites in the same zone might be important for these neurites to establish proper zonal innervation patterns. However, our results suggest that the targeting and elaboration networks of DAN axons and MBON dendrites are largely independent, at least for those projecting to the MB vertical lobes. In the α′2 zone, where innervation by DAN axons precedes that by MBON dendrites, ablation of DANs does not affect zonal elaboration of the MBON dendrites. Moreover, upon ablation of one type of DAN or MBON in a given zone, morphologies of the neighboring neurites appear to be normal. Therefore, the extent and location of zonal network elaboration by DAN axons and MBON dendrites in the vertical lobes do not depend on interactions between these extrinsic neurons.

The importance of the KCs. In each MB lobe zone, the DAN axons and MBON dendrites form synapses with each other and the KC axons (18, 55, 56). Given that DANs and MBONs do not depend on each other to form zonal networks, could KCs be responsible? Our results support the importance of the KCs in the zonal organization of the DAN axons and MBON dendrites. Aberrant branching of KCs in *ala* mutant brains resulted in some MBs lacking the vertical lobes. When this occurred, most DAN axons and MBON dendrites that normally innervate these lobes do not form zonal arborization (Fig. 3). Without the MB vertical lobes, MBON-α′2 dendrites are rerouted to other zones in the horizontal lobes and form potential synaptic connections with the local DAN axons (Fig. 3 *C–G*). Importantly, this reorganization of the MBON dendrites requires the presence of the KCs (Fig. 3 *H* and *I*).

It is still possible that the KC axons and the lobes they form simply provide an anchoring point on which DAN axons and MBON dendrites grow, and that the extent of their arborization is determined cell-autonomously as an intrinsic property. However, the axonal innervation pattern of PPL1 DANs argues against this possibility. PPL1-α′3 and PPL1-α′2α2 axons enter the MB vertical lobes at almost the same location but specifically occupy distinct zones on opposite sides of the entry point (*SI Appendix*, Fig. S6 *K–K′*), suggesting the existence of local positional cues in the lobes to guide the innervation of DAN axons. Furthermore, overexpression of *sema1a* in DANs directs their dendrites to specific MB lobe zones, and importantly, the arborization of these rerouted dendrites is confined to their respective zones (Fig. 5 *A–H*). Since these DAN dendrites normally do not innervate the MB lobe, there likely exist local positional cues that interact with Sema1a-expressing dendrites to guide their zonal arborization.

What could be the sources of these positional cues? KCs are good candidates because they synapse with DAN axons and MBON dendrites and are essential for zonal arborization of

these neurites. However, since KCs provide the main framework of the MB lobes, their manipulation may affect the organization of other cell types in the MB lobes that could also be potential sources of the positional cues. Electron microscopy-based reconstructions of the MB circuit have provided a comprehensive catalog for the neurons that innervate the MB lobe (18, 56). In addition to KCs, DANs, and MBONs, the MB lobes are innervated by one dorsal paired medial (DPM) neuron, one anterior paired lateral (APL) neuron, two SIFamide-expressing neurons, and two octopaminergic neurons. These neurons do not exhibit zonal innervation patterns in the MB lobes; the SIFamide- and octopamine-expressing neurons only sparsely innervate the MB lobes, and the neurites of APL and DPM ramify the entire MB lobes. The MB lobes are also populated by glia, which is another potential source of the positional cues (57). Although their sources remain undetermined, our results suggest that the MB lobes are likely prepatterned with positional cues to guide the zonal elaboration of the MBON and DAN neurites.

Sema1a and Wiring of the MB Circuit. Sema1a is an evolutionarily conserved guidance molecule that functions as a ligand or receptor depending on the cellular context (28, 42, 45, 50–52, 58). Our data suggest that Sema1a functions as a receptor in MBONs to regulate dendritic targeting in a zone-specific manner. Loss of *sema1a* activity preferentially affects MBON dendrites in the α′3, α′1, and β′2 zones. Even for MBONs that innervate multiple zones, such as MBON-β2β′2a and MBON-γ5β′2a, reducing *sema1a* activity in these neurons selectively impacts their dendrites in the β′2a zone (Fig. 4 *A* and *B* and *SI Appendix*, Fig. S9 *C–D′*). Since Sema1a is not differentially localized in the dendrites of these MBONs (*SI Appendix*, Fig. S8 *D–F′*, *M*, and *N*), the guidance cues that Sema1a responds to might primarily be present in the β′2a zone, with additional guidance signals working collaboratively to sort the dendrites from these MBONs into Sema1a-sensitive and -insensitive zones. Not all MBONs innervating these Sema1a-sensitive zones require Sema1a. For MBON-γ2α′1 and MBON-α′1 that both innervate the α′1 zone, loss of *sema1a* only affects dendritic innervation by MBON-α′1 but not MBON-γ2α′1 (*SI Appendix*, Fig. S9 *G–J*). Therefore, how Sema1a functions is also cell-type-specific. Taken together, these results imply that multiple positional cues may be present in each MB lobe zone, with each MBON being equipped with multiple sensors that work in concert to respond to those cues. Moreover, given that Sema1a is broadly expressed in many neurons in the developing brain, including the KCs, Sema1a likely acts with other proteins or signaling molecules to determine guidance specificity (*SI Appendix*, Video S1) (59).

Sema1a has been shown to mediate both neurite attraction and avoidance (60). Currently, it is unclear which of the two mechanisms underlies its guidance of MBON dendrites. For MBONs whose zonal dendritic innervation requires *sema1a*, their dendrites can still project to areas nearby their target zones when *sema1a* activity was removed (Fig. 4 and *SI Appendix*, Fig. S9). Hence, the cues that guide these MBON dendrites are likely to be short-ranged. However, overexpression of *sema1a* in PPL1-α′2α2 DANs can redirect their dendrites to innervate zones far away from their original location, suggesting that the guidance cues may also exert long-distance functionality. Our data indicate that Sema1a functions as a receptor in MBONs. Identification of Sema1a ligands and determining their distributions in the MB lobes are critical steps toward understanding how Sema1a instructs the zonal innervation of MBON dendrites. Plexin A (PlexA) or secreted Semaphorin 2a and 2b (Sema2a and Sema2b) are known ligands for the Sema1a receptor (42, 51, 52). We have tested if these canonical ligands of Sema1a are required for the dendritic innervations of β′2- and α′3-projecting MBONs. However, dendritic innervations by these MBONs were minimally affected in homozygous *sema2a/2b* double mutant flies or when we knocked down PlexA either pan-neuronally or in glia (*SI Appendix*, Fig. S11). Therefore, the canonical Sema1a ligands do not seem to play a role in MBON dendritic targeting. However, it remains to be determined if PlexA and Sema2a/2b function redundantly in this system or if an unidentified noncanonical ligand is involved.

A Working Model for Combinatorial Coding of Guidance Cues in MB Assembly. Although the molecular nature of the positional cues in the MB lobes that organize the zonal patterns of DAN and MBON neurites awaits discovery, our data suggest that these cues likely work in a combinatorial manner. Supporting evidence for this notion comes from our observation that MBON-α′1 and MBON-γ2α′1 use *sema1a*-dependent and -independent mechanisms to innervate the α′1 zone, indicating that this zone may present at least two different guidance cues (*SI Appendix*, Fig. S9 *G–J*). Furthermore, *sema1a* is expressed in multiple MBONs that innervate distinct MB lobe zones. This pattern could potentially be explained if the positional cues attracting Sema1a-positive neurites appear sequentially in these zones (i.e., so that the zone an MBON innervates is determined by the developmental timing of the MBON). However, our finding that the ectopic innervations of MBON-α′2 in the β′2 and α′1-like zones of the *ala* brain occur simultaneously argues against that possibility (*SI Appendix*, Fig. S7 *D–D′*). Therefore, the Sema1a-sensitive zones likely harbor additional zone-specific guidance cues that work in combination with Sema1a to diversify guidance specificity.

Our observation that the mistargeted MBON-α′2 dendrites in *ala* mutant brains innervate other zones in the α′β′ lobe, but not those in the αβ and γ lobes (Fig. 3*C*), has also prompted us to hypothesize that there might be general attraction cues emanating from the α′β′ lobes for all α′β′ lobe-projecting MBONs, separating them from MBONs targeting αβ and γ lobes. Therefore, herein we propose a hypothetical model whereby multiple hierarchically-organized positional cues are presented in the MB lobe zones, with these cues acting in concert to pattern zonal innervation by DAN axons and MBON dendrites in the MB lobes (Fig. 5*I*).

Materials and Methods

Fly Strains and Husbandry. Fly lines used in this study are shown in *SI Appendix*, Table S2. The genotypes of the flies used in each figure are shown in *SI Appendix*, Table S3. All flies were reared at 23 °C with 60% relative humidity, under a 12:12 h light:dark cycle. All our data are derived from male flies.

MARCM and Flip-Out. Flies of desired genotype were heat-shocked at 37 °C at different developmental stages for different durations (see *SI Appendix*, Table S3 for each of these parameters used in each figure). For flip-out clones induced at the adult stage, we waited for at least 3 d after heat-shock to ensure proper expression of the marker proteins. Brains were then dissected for immunofluorescence staining.

Immunofluorescence Staining. Fly brains were dissected and stained following the procedure in our previous study (13). See detailed information in *SI Appendix, Supplementary Methods*.

Hydroxyurea Feeding. Fly larvae within 1 h of hatching were fed with 50 mg/mL hydroxyurea mixed with heat-inactivated yeast for 4 h. The larvae were then

transferred to normal food vials until they became 3- to 4-d-old adults. The flies were dissected to examine their MB neurons. See a more detailed protocol in *SI Appendix, Supplementary Methods*.

Statistics. Statistical analysis was performed in Prism 8 (GraphPad, CA, USA). All data were tested for normality using the Shapiro-Wilk normality test. No datapoints were excluded from our analyses. Since all our data are normally distributed, we used two-tailed unpaired Student's *t* test when comparing two datasets and one-way ANOVA with Tukey's multiple comparisons test when comparing three or more datasets. To compare categorical data, we used Fisher's exact test. All hemibrains were considered independent samples.

Data Availability. All study data are included in the article and/or *SI Appendix*.

ACKNOWLEDGMENTS. We thank S. Waddell, E. Perisse, and all Lin Lab members for commenting on the manuscript. We also thank Y. Aso, C.H. Lee, T. Lee, L. Luo, G. Rubin, Y.-H. Sun, S. Waddell, C.-L. Wu, H.-H. Yu, and L. Zipursky for sharing reagents and fly lines. Thanks are also due to FlyLight, the Bloomington Drosophila Stock Center, Vienna Drosophila RNAi Center, Harvard TRiP RNAi Stock Center, Kyoto Stock Center, and Taiwan Fly Core for providing fly stocks. S.L. is funded by the Taiwan Ministry of Science and Technology (107-2311-B-001-042-MY3 and 109-2628-B-001-013) and Academia Sinica, Taiwan.

1. J. S. de Belle, M. Heisenberg, Associative odor learning in Drosophila abolished by chemical ablation of mushroom bodies. *Science* **263**, 692–695 (1994).
2. M. Heisenberg, Mushroom body memoir: From maps to models. *Nat. Rev. Neurosci.* **4**, 266–275 (2003).
3. Y. Aso *et al.*, The neuronal architecture of the mushroom body provides a logic for associative learning. *eLife* **3**, e04577 (2014).
4. D. Owald, S. Waddell, Olfactory learning skews mushroom body output pathways to steer behavioral choice in Drosophila. *Curr. Opin. Neurobiol.* **35**, 178–184 (2015).
5. M. Adel, L. C. Griffith, The role of dopamine in associative learning in Drosophila: An updated unified model. *Neurosci. Bull.* **37**, 831–852 (2021).
6. W. J. Joiner, A. Crocker, B. H. White, A. Sehgal, Sleep in Drosophila is regulated by adult mushroom bodies. *Nature* **441**, 757–760 (2006).
7. J. L. Pitman, J. J. McGill, K. P. Keegan, R. Allada, A dynamic role for the mushroom bodies in promoting sleep in Drosophila. *Nature* **441**, 753–756 (2006).
8. J. Lim *et al.*, The mushroom body D1 dopamine receptor controls innate courtship drive. *Genes Brain Behav.* **17**, 158–167 (2018).
9. S. A. Montague, B. S. Baker, Memory elicited by courtship conditioning requires mushroom body neuronal subsets similar to those utilized in appetitive memory. *PLoS One* **11**, e0164516 (2016).
10. K. Keleman *et al.*, Dopamine neurons modulate pheromone responses in Drosophila courtship learning. *Nature* **489**, 145–149 (2012).
11. M. J. Krashes *et al.*, A neural circuit mechanism integrating motivational state with memory expression in Drosophila. *Cell* **139**, 416–427 (2009).
12. C. H. Tsao, C. C. Chen, C. H. Lin, H. Y. Yang, S. Lin, *Drosophila* mushroom bodies integrate hunger and satiety signals to control innate food-seeking behavior. *eLife* **7**, e35264 (2018).
13. B. Senapati *et al.*, A neural mechanism for deprivation state-specific expression of relevant memories in Drosophila. *Nat. Neurosci.* **22**, 2029–2039 (2019).
14. S. Sayin *et al.*, A neural circuit arbitrates between persistence and withdrawal in hungry Drosophila. *Neuron* **104**, 544–558.e6 (2019).
15. G. Laurent, Olfactory network dynamics and the coding of multidimensional signals. *Nat. Rev. Neurosci.* **3**, 884–895 (2002).
16. A. Litwin-Kumar, K. D. Harris, R. Axel, H. Sompolinsky, L. F. Abbott, Optimal degrees of synaptic connectivity. *Neuron* **93**, 1153–1164.e7 (2017).
17. S. M. Farris, Are mushroom bodies cerebellum-like structures? *Arthropod Struct. Dev.* **40**, 368–379 (2011).
18. F. Li *et al.*, The connectome of the adult Drosophila mushroom body provides insights into function. *eLife* **9**, e62576 (2020).
19. J. R. Crittenden, E. M. Skoulakis, K. A. Han, D. Kalderon, R. L. Davis, Tripartite mushroom body architecture revealed by antigenic markers. *Learn. Mem.* **5**, 38–51 (1998).
20. N. Kim, S. J. Burden, MuSK controls where motor axons grow and form synapses. *Nat. Neurosci.* **11**, 19–27 (2008).
21. F. Ango *et al.*, Ankyrin-based subcellular gradient of neurofascin, an immunoglobulin family protein, directs GABAergic innervation at purkinje axon initial segment. *Cell* **119**, 257–272 (2004).
22. J. R. Sanes, M. Yamagata, Many paths to synaptic specificity. *Annu. Rev. Cell Dev. Biol.* **25**, 161–195 (2009).
23. K. Ito, W. Awano, K. Suzuki, Y. Hiromi, D. Yamamoto, The Drosophila mushroom body is a quadruple structure of clonal units each of which contains a virtually identical set of neurones and glial cells. *Development* **124**, 761–771 (1997).
24. T. Lee, A. Lee, L. Luo, Development of the Drosophila mushroom bodies: Sequential generation of three distinct types of neurons from a neuroblast. *Development* **126**, 4065–4076 (1999).
25. K. Eichler *et al.*, The complete connectome of a learning and memory centre in an insect brain. *Nature* **548**, 175–182 (2017).
26. T. Saumweber *et al.*, Functional architecture of reward learning in mushroom body extrinsic neurons of larval Drosophila. *Nat. Commun.* **9**, 1104 (2018).
27. B. Bornstein *et al.*, Transneuronal Dpr12/DIP-δ interactions facilitate compartmentalized dopaminergic innervation of Drosophila mushroom body axons. *EMBO J.* **40**, e105763 (2021).
28. A. L. Kolodkin, D. J. Matthes, C. S. Goodman, The semaphorin genes encode a family of transmembrane and secreted growth cone guidance molecules. *Cell* **75**, 1389–1399 (1993).
29. A. Nern, B. D. Pfeiffer, G. M. Rubin, Optimized tools for multicolor stochastic labeling reveal diverse stereotyped cell arrangements in the fly visual system. *Proc. Natl. Acad. Sci. U.S.A.* **112**, E2967–E2976 (2015).
30. W. S. Neckameyer, W. G. Quinn, Isolation and characterization of the gene for Drosophila tyrosine hydroxylase. *Neuron* **2**, 1167–1175 (1989).
31. M. E. Grether, J. M. Abrams, J. Agapite, K. White, H. Steller, The head involution defective gene of Drosophila melanogaster functions in programmed cell death. *Genes Dev.* **9**, 1694–1708 (1995).
32. K. White *et al.*, Genetic control of programmed cell death in Drosophila. *Science* **264**, 677–683 (1994).
33. H. Wässle, L. Peichl, B. B. Boycott, Dendritic territories of cat retinal ganglion cells. *Nature* **292**, 344–345 (1981).
34. W. B. Grueber, L. Y. Jan, Y. N. Jan, Tiling of the Drosophila epidermis by multidendritic sensory neurons. *Development* **129**, 2867–2878 (2002).
35. A. Pascual, M. Chaminade, T. Préat, Ethanolamine kinase controls neuroblast divisions in Drosophila mushroom bodies. *Dev. Biol.* **280**, 177–186 (2005).
36. A. Pascual, T. Préat, Localization of long-term memory within the Drosophila mushroom body. *Science* **294**, 1115–1117 (2001).
37. L. J. Nicolaï *et al.*, Genetically encoded dendritic marker sheds light on neuronal connectivity in Drosophila. *Proc. Natl. Acad. Sci. U.S.A.* **107**, 20553–20558 (2010).
38. D. Owald *et al.*, A Syd-1 homologue regulates pre- and postsynaptic maturation in Drosophila. *J. Cell Biol.* **188**, 565–579 (2010).
39. E. H. Feinberg *et al.*, GFP Reconstitution Across Synaptic Partners (GRASP) defines cell contacts and synapses in living nervous systems. *Neuron* **57**, 353–363 (2008).
40. S. Lin *et al.*, Neural correlates of water reward in thirsty Drosophila. *Nat. Neurosci.* **17**, 1536–1542 (2014).
41. J. Timson, Hydroxyurea. *Mutat. Res.* **32**, 115–132 (1975).
42. S. Jeong, K. Juhaszova, A. L. Kolodkin, The Control of semaphorin-1a-mediated reverse signaling by opposing pebble and RhoGAPp190 functions in drosophila. *Neuron* **76**, 721–734 (2012).
43. T. Komiyama, L. B. Sweeney, O. Schuldiner, K. C. Garcia, L. Luo, Graded expression of semaphorin-1a cell-autonomously directs dendritic targeting of olfactory projection neurons. *Cell* **128**, 399–410 (2007).
44. T. A. Godenschwege, H. Hu, X. Shan-Crofts, C. S. Goodman, R. K. Murphey, Bi-directional signaling by Semaphorin 1a during central synapse formation in Drosophila. *Nat. Neurosci.* **5**, 1294–1301 (2002).
45. H. H. Yu, H. H. Araj, S. A. Ralls, A. L. Kolodkin, The transmembrane Semaphorin Sema I is required in Drosophila for embryonic motor and CNS axon guidance. *Neuron* **20**, 207–220 (1998).
46. H. H. Hsieh, W. T. Chang, L. Yu, Y. Rao, Control of axon-axon attraction by Semaphorin reverse signaling. *Proc. Natl. Acad. Sci. U.S.A.* **111**, 11383–11388 (2014).
47. S. Sasse, C. Klämbt, Repulsive epithelial cues direct glial migration along the nerve. *Dev. Cell* **39**, 696–707 (2016).
48. M. Y. Pecot *et al.*, Multiple interactions control synaptic layer specificity in the Drosophila visual system. *Neuron* **77**, 299–310 (2013).
49. L. A. Perkins *et al.*, The transgenic RNAi Project at Harvard Medical School: Resources and validation. *Genetics* **201**, 843–852 (2015).
50. M. L. Winberg *et al.*, Plexin A is a neuronal semaphorin receptor that controls axon guidance. *Cell* **95**, 903–916 (1998).
51. P. Cafferty, L. Yu, H. Long, Y. Rao, Semaphorin-1a functions as a guidance receptor in the Drosophila visual system. *J. Neurosci.* **26**, 3999–4003 (2006).
52. L. B. Sweeney *et al.*, Secreted semaphorins from degenerating larval ORN axons direct adult projection neuron dendrite targeting. *Neuron* **72**, 734–747 (2011).
53. T. Lee, L. Luo, Mosaic analysis with a repressible cell marker for studies of gene function in neuronal morphogenesis. *Neuron* **22**, 451–461 (1999).
54. L. J. Macpherson *et al.*, Dynamic labelling of neural connections in multiple colours by trans-synaptic fluorescence complementation. *Nat. Commun.* **6**, 10024 (2015).
55. I. Cervantes-Sandoval, A. Phan, M. Chakraborty, R. L. Davis, Reciprocal synapses between mushroom body and dopamine neurons form a positive feedback loop required for learning. *eLife* **6**, e23789 (2017).
56. S. Y. Takemura *et al.*, A connectome of a learning and memory center in the adult *Drosophila* brain. *eLife* **6**, e26975 (2017).
57. M. C. Kremer, C. Jung, S. Batelli, G. M. Rubin, U. Gaul, The glia of the adult Drosophila nervous system. *Glia* **65**, 606–638 (2017).
58. R. J. Pasterkamp, Getting neural circuits into shape with semaphorins. *Nat. Rev. Neurosci.* **13**, 605–618 (2012).
59. L. Zwarts, T. Goossens, J. Clements, Y. Y. Kang, P. Callaerts, Axon branch-specific Semaphorin-1a signaling in Drosophila mushroom body development. *Front. Cell. Neurosci.* **10**, 210 (2016).
60. M. Hernandez-Fleming, E. W. Rohrbach, G. J. Bashaw, Sema-1a reverse signaling promotes midline crossing in response to secreted Semaphorins. *Cell Rep.* **18**, 174–184 (2017).